CM11v251015wed

2025년 9월 18일 목요일 09:51

Multiple-stream decomposition

where the Hermitian transpose of the blocking matrix $\boldsymbol{B}(f)$ is defined as

$$\boldsymbol{B}(f)^{\mathcal{H}} \triangleq \begin{bmatrix} \boldsymbol{w}_{1,0}(f)^{\mathcal{H}}\boldsymbol{H}_1(f) \\ \boldsymbol{w}_{1,1}(f)^{\mathcal{H}}\boldsymbol{H}_1(f) \\ \vdots \\ \boldsymbol{w}_{1,M_0M_1-1}(f)^{\mathcal{H}}\boldsymbol{H}_1(f) \\ \vdots \\ \boldsymbol{w}_{K,0}(f)^{\mathcal{H}}\boldsymbol{H}_K(f) \\ \boldsymbol{w}_{K,1}(f)^{\mathcal{H}}\boldsymbol{H}_K(f) \\ \vdots \\ \boldsymbol{w}_{K,M_0M_K-1}(f)^{\mathcal{H}}\boldsymbol{H}_K(f) \\ \hat{\boldsymbol{w}}_{-L}(f)^{\mathcal{H}} \\ \hat{\boldsymbol{w}}_{-L+1}(f)^{\mathcal{H}} \\ \vdots \\ \hat{\boldsymbol{w}}_{L}(f)^{\mathcal{H}} \end{bmatrix} \tag{27}$$

with the VFTs $\hat{\boldsymbol{w}}_l(f), l = -L, -L+1, ..., L$, of the receive waveforms of the virtual legacy receivers augmenting the orthogonality constraint (21b).

IV. Optimal Solution and Its Existence

In this section, the optimal solution to *Problem 2* with the modified zero-interference constraint (26) is derived. Due to the constraint (26), it is possible for the constraint set to be empty, which makes the problem vacuous. So, a natural question is when *Problem 2* has an optimal solution. This issue of the existence of the solution is also discussed.

A. Derivation of Optimal Solution

The optimization problem *Problem 2* can be rewritten in a double minimization form

$$\underset{\boldsymbol{s}(f)}{\text{minimize}}\left\{\min_{\boldsymbol{w}(f)}\int_{\mathcal{F}} TM(fT) + \boldsymbol{w}(f)^{\mathcal{H}}\boldsymbol{R}_Z(f)\boldsymbol{w}(f) - 2\Re\Big(\boldsymbol{w}(f)^{\mathcal{H}}\big(M(fT)\boldsymbol{p}(f)\big)\Big)df\right\}, \tag{28}$$

with the constraints (26) and (21c) being imposed not on the inner minimization but only on the outer minimization. Since the inner minimization reduces to finding the linear minimum mean-squared error (LMMSE) receiver without any constraint, the solution can be easily found as [11]

$$\boldsymbol{w}_{\text{lmmse}}(f) = \frac{M(fT)\boldsymbol{R}_N(f)^{-1}\boldsymbol{H}(f)\boldsymbol{s}(f)}{1+\frac{M(fT)}{T}\boldsymbol{s}(f)^{\mathcal{H}}\boldsymbol{C}(f)\boldsymbol{s}(f)}, \forall f \in \mathcal{F}, \tag{29}$$

where $\boldsymbol{H}(f)$ is the $\mathcal{N}(f)$-by-$\mathcal{N}(f)$ diagonal matrix defined as

$$\boldsymbol{H}(f) \triangleq \text{diag}(\boldsymbol{h}(f)) \tag{30}$$

and $\boldsymbol{C}(f)$ is the $\mathcal{N}(f)$-by-$\mathcal{N}(f)$ matrix-valued frequency function given by

$$\boldsymbol{C}(f) \triangleq \boldsymbol{H}(f)^{\mathcal{H}}\boldsymbol{R}_N(f)^{-1}\boldsymbol{H}(f) \tag{31}$$

because $\boldsymbol{w}_{\text{lmmse}}(f) = \boldsymbol{0}, \forall f \in (\mathcal{F}_M)^c$.

Now, the outer minimization problem reduces to finding $\boldsymbol{s}(f)$ that minimizes the MSE in (32) subject to the constraints (26) and (21c). To proceed, we define the energy density function $a(f)$ of $\boldsymbol{s}(f)$ as [11]

$$a(f) \triangleq \boldsymbol{s}(f)^{\mathcal{H}}\boldsymbol{s}(f) \tag{33}$$

for $f \in \mathcal{F}$. Then, the constraint set can be partitioned into subsets, each of which contains all feasible $\boldsymbol{s}(f)$ having the same energy density function $a(f)$. So, the outer minimization problem can be rewritten in an equivalent double minimization form

Problem 3:

$$\underset{a(f)}{\text{minimize}}\begin{cases}\min\limits_{\boldsymbol{s}(f)}\int_{\mathcal{F}_M}\frac{TM(fT)}{1+\frac{M(fT)}{T}\boldsymbol{s}(f)^{\mathcal{H}}\boldsymbol{C}(f)\boldsymbol{s}(f)}df, \\ \text{subject to } \boldsymbol{B}(f)^{\mathcal{H}}\boldsymbol{s}(f) = \boldsymbol{0}, \forall f \in \mathcal{F}_M, \\ \qquad \boldsymbol{s}(f)^{\mathcal{H}}\boldsymbol{s}(f) = a(f), \forall f \in \mathcal{F}_M,\end{cases}$$

$$\text{subject to} \int_{\mathcal{F}_M}\frac{M(fT)}{T}a(f)df = A. \tag{34}$$

This shows again that an arbitrary choice of the optimal transmit waveform $\boldsymbol{s}_{\text{opt}}(f)$ will do for $f \in (\mathcal{F}_M)^c$.

To minimize the objective function of the inner optimization problem of *Problem 3*, we need to find $\boldsymbol{s}_{\text{opt}}(f)$ that maximizes the denominator of the integrand at each $f \in \mathcal{F}_M$. Hence, the inner optimization problem to find $\boldsymbol{s}_{\text{opt}}(f)$ given $a(f)$ now reduces to a *convex maximization* problem

Sub-Problem 1:

$$\underset{\boldsymbol{s}(f)}{\text{maximize}}\ \boldsymbol{s}(f)^{\mathcal{H}}\boldsymbol{C}(f)\boldsymbol{s}(f) \tag{35a}$$

$$\text{subject to } \boldsymbol{B}(f)^{\mathcal{H}}\boldsymbol{s}(f) = \boldsymbol{0}, \tag{35b}$$

$$\boldsymbol{s}(f)^{\mathcal{H}}\boldsymbol{s}(f) = a(f), \tag{35c}$$

which needs to be solved for each $f \in \mathcal{F}_M$. This problem can be interpreted as an optimal beamforming problem that must generate orthogonal beams to legacy receivers at each frequency offset f.

In [18] and [19], solutions to some unusual eigenvalue problems are provided, where non-VFT version of *Sub-Problem 1* is solved for real-valued vectors and matrices with $a(f)$ being unity and the matrix $\boldsymbol{B}(f)$ being of full rank. The following proposition extends this solution to our case. To proceed, we define the projection matrix $\boldsymbol{P}_{\boldsymbol{B}}(f)$ and the orthogonal projection matrix $\boldsymbol{P}_{\boldsymbol{B}}^{\perp}(f)$ of $\boldsymbol{B}(f)$ as

$$\boldsymbol{P}_{\boldsymbol{B}}(f) \triangleq \boldsymbol{B}(f)\left(\boldsymbol{B}(f)^{\mathcal{H}}\boldsymbol{B}(f)\right)^{\dagger}\boldsymbol{B}(f)^{\mathcal{H}}, \tag{36a}$$

and

$$\boldsymbol{P}_{\boldsymbol{B}}^{\perp}(f) \triangleq \boldsymbol{I}_{\mathcal{N}(f)} - \boldsymbol{P}_{\boldsymbol{B}}(f), \tag{36b}$$

respectively, where $\boldsymbol{I}_{\mathcal{N}(f)}$ denotes the $\mathcal{N}(f)$-by-$\mathcal{N}(f)$ identity matrix and † denotes Moore-Penrose generalized inverse.

Proposition 1: The optimal solution $\boldsymbol{s}_{\text{opt}}(f)$ to *Sub-Problem 1* is given by

$\square$ $\underline{s} \in \mathbb{C}^{3\times 1}$

$\max\limits_{\underline{s}}\ \underline{s}^H R\,\underline{s}$

s.t. $\|\underline{s}\| = 1$

$\underline{s}^H \underline{e}_1 = 0.$

$\boxed{\underline{e}}^H \underline{s}$

$\begin{bmatrix} 0 \\ \square \\ \square \end{bmatrix}$

B

$\equiv \max\limits_{\underline{s}}\ \underline{s}^H \tilde{R}\,\underline{s}$

s.t. $\|\underline{s}\| = 1$

$\underline{b}_1^H \underline{s} = 0$

$\underline{b}_2^H \underline{s} = 0$

$\equiv B^H \underline{s} = \underline{0}_2$

when $B = [\underline{b}_1\ \underline{b}_2]$

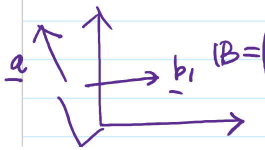

$\mathbb{B} = [\underline{b}_1\ \underline{b}_2]$

$$\mathbf{H}(f) \triangleq \mathrm{diag}(\mathbf{h}(f)) \tag{30}$$

and $\mathbf{C}(f)$ is the $\mathcal{N}(f)$-by-$\mathcal{N}(f)$ matrix-valued frequency function given by

$$\mathbf{C}(f) \triangleq \mathbf{H}(f)^{\mathcal{H}}\mathbf{R}_N(f)^{-1}\mathbf{H}(f). \tag{31}$$

With this solution (29), the MSE performance is given by

$$\int_{\mathcal{F}_M} \frac{TM(fT)}{1+\frac{M(fT)}{T}\mathbf{s}(f)^{\mathcal{H}}\mathbf{C}(f)\mathbf{s}(f)}df, \tag{32}$$

respectively, where $\mathbf{I}_{\mathcal{N}(f)}$ denotes the $\mathcal{N}(f)$-by-$\mathcal{N}(f)$ identity matrix and † denotes Moore-Penrose generalized inverse.

Proposition 1: The optimal solution $\mathbf{s}_{\text{opt}}(f)$ to *Sub-Problem 1* is given by

$$\mathbf{s}_{\text{opt}}(f) = \sqrt{a(f)}\mathbf{v}_{\max}(f)e^{j\theta(f)} \tag{37}$$

for $f \in \mathcal{F}_M$, where $\theta(f)$ can be chosen arbitrarily and $\mathbf{v}_{\max}(f)$ is the normalized eigenvector corresponding to the largest eigenvalue $\lambda_{\max}(f)$ of $\mathbf{P}_{\mathbf{B}}^{\perp}(f)\mathbf{C}(f)$.

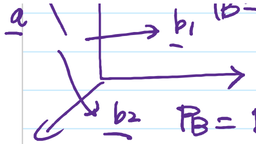

$P_B = B(B^H B)^{-1} B^H$

$P_B^{\perp} = I - B(B^H B)^{-1} B^H$

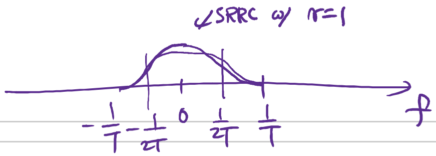

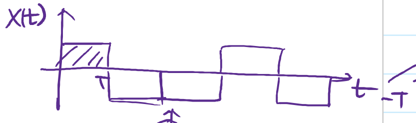

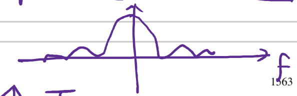

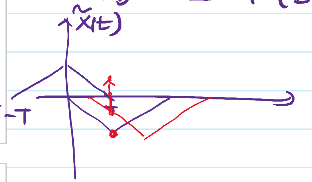

Y(t) T t

Proof: See Appendix B. □

As shown in the proof of *Proposition 1*, the maximum value of the objective function is given by $\lambda_{\max}(f)\mathbf{s}_{\text{opt}}(f)^{\mathcal{H}}\mathbf{s}_{\text{opt}}(f) = a(f)\lambda_{\max}(f)$ for $f \in \mathcal{F}_M$. Thus, the outer minimization of *Problem 3* to find the optimal energy allotment $a_{\text{opt}}(f)$ for $f \in \mathcal{F}_M$ becomes

Sub-Problem 2:

$$\underset{a(f)}{\text{minimize}} \int_{\mathcal{F}_M} \frac{TM(fT)}{1+\frac{M(fT)}{T}\lambda_{\max}(f)a(f)}df$$
$$\text{subject to} \int_{\mathcal{F}_M} \frac{M(fT)}{T}a(f)df = A. \tag{38}$$

Now, the result in [11] can be used in obtaining the following solution to *Problem 2*, since *Sub-Problem 2* to find the optimal energy allotment $a_{\text{opt}}(f)$ for $f \in \mathcal{F}_M$ is the same problem as the one in [11, Eq. (44)] only except that $\mathcal{F}$ is now replaced by $\mathcal{F}_M$ and that the orthogonality constraint (26) has changed $\lambda_{\max}(f)$ from the largest eigenvalue of $\mathbf{C}(f)$ to the largest eigenvalue of $\mathbf{P}_{\mathbf{B}}^{\perp}(f)\mathbf{C}(f)$, so that $\lambda_{\max}(f)$ can be zero for some f. To proceed, we define the set

$$\mathcal{F}_{\lambda_{\max}} \triangleq \{f \in \mathcal{F} : \lambda_{\max}(f) \neq 0\}, \tag{39}$$

as the support of $\lambda_{\max}(f)$.

Theorem 1: The VFTs $\mathbf{s}_{\text{opt}}(f)$ and $\mathbf{w}_{\text{opt}}(f)$ of the jointly optimal transmit waveform $s_{\text{opt}}(t)$ and the receive waveform $w_{\text{opt}}(t)$ as the solutions to *Problem 2* are given, respectively, by

$$\mathbf{s}_{\text{opt}}(f) = \begin{cases} \sqrt{a_{\text{opt}}(f)}\mathbf{v}_{\max}(f)e^{j\theta(f)}, & \forall f \in \mathcal{F}_M, \\ \text{arbitrary}, & \forall f \in (\mathcal{F}_M)^c \end{cases} \tag{40}$$

and

$$\mathbf{w}_{\text{opt}}(f) = \frac{M(fT)\mathbf{R}_N(f)^{-1}\mathbf{H}(f)\mathbf{s}_{\text{opt}}(f)}{1+\frac{M(fT)}{T}\lambda_{\max}(f)a_{\text{opt}}(f)}, \quad \forall f \in \mathcal{F}, \tag{41}$$

where the optimal energy allotment $a_{\text{opt}}(f)$ is given by

$$a_{\text{opt}}(f) = \left[\nu_{\text{opt}} - \sqrt{\frac{T}{M(fT)\lambda_{\max}(f)}}\right]^+ \sqrt{\frac{T}{M(fT)\lambda_{\max}(f)}}, \tag{42}$$

for $f \in \mathcal{F}_M \cap \mathcal{F}_{\lambda_{\max}}$ with $\nu_{\text{opt}} > 0$ being the unique solution to

$$\int_{\mathcal{F}_M \cap \mathcal{F}_{\lambda_{\max}}} \left[\nu_{\text{opt}} - \sqrt{\frac{T}{M(fT)\lambda_{\max}(f)}}\right]^+ \sqrt{\frac{M(fT)}{T\lambda_{\max}(f)}}df = A, \tag{43}$$

and $[x]^+ \triangleq \max(x, 0)$ denoting the positive part of x, and $a_{\text{opt}}(f) = 0$ for $f \in \mathcal{F}_M \cap (\mathcal{F}_{\lambda_{\max}})^c$.

Proof: See Appendix C. □

The solution found in *Theorem 1* leads to the jointly minimized MSE ε_{opt} given by

B. A Necessary and Sufficient Condition for Existence of Solution

The final question to be answered is what is the necessary and sufficient condition for the existence of a non-trivial optimal solution such that $\varepsilon_{\text{opt}} < \mathbb{E}\{|b[l]|^2\} = \int_{\mathcal{F}_M} TM(fT)df$. In this subsection, we show that the existence of a non-trivial optimal solution can be determined solely by the orthogonality constraint (26). To proceed, we prove the following lemma. Note that the result is not trivial because $\mathbf{C}(f)$ is positive *semi-definite* in general.

Lemma 2:

$$\mathbf{P}_{\mathbf{B}}^{\perp}(f) = \mathbf{0} \Longleftrightarrow \boxed{\mathbf{P}_{\mathbf{B}}^{\perp}(f)\mathbf{C}(f)\mathbf{P}_{\mathbf{B}}^{\perp}(f) = \mathbf{0}.} \tag{45}$$

Proof: See Appendix D. □

Theorem 2: A non-trivial optimal solution exists if and only if (iff) the length of the set

$$\left\{f \in \mathcal{F}_M : \mathrm{Dim}\left(\text{null space of } \mathbf{B}(f)^{\mathcal{H}}\right) > 0\right\} \tag{46}$$

is greater than zero, where $\mathrm{Dim}(\cdot)$ denotes the dimension of a subspace.

Proof: See Appendix E. □

The above result provides a simple way to perform admission control without performing eigen-decomposition of the matrix $\mathbf{P}_{\mathbf{B}}^{\perp}(f)\mathbf{C}(f)$ but just using the matrix $\mathbf{B}(f)$ that can be obtained once the frequency responses and the sampling timings of the legacy and the virtual legacy receivers are identified.

V. Numerical Results

In this section, we provide numerical results that demonstrate the effectiveness of our solution in designing overlay systems. The Monte-Carlo integration results as well as the bit error rate (BER) estimates based on the conditional Gaussian approximation (See [20] and references therein.) of the overall interference are provided. Throughout this section, the legacy and the overlay systems employ linear modulation with QPSK symbols. The legacy transmitters have square-root raised cosine transmit waveforms with roll-off factor $\gamma \in [0, 1]$. For simplicity, all the channels to the legacy receivers are chosen to be frequency flat, and the legacy receivers employ matched filters followed by symbol rate samplers.

The first results are to compare the performance of the proposed overlay system with that of the overlay system utilizing guard bands only. There are four legacy systems with $\gamma = 0.2$, and the length of each guard band is $0.2/T_0$. The overlay systems with $1/T = 1/T_0$ are to be designed. For illustrative purpose, the channels to the overlay Rx are chosen to be two-path frequency selective channels with impulse responses $h_1(t) = 0.9e^{j\frac{\pi}{4}}\delta(t - T_0/8) + 0.4\delta(t - 15T_0/16)$, and $[x]^+ \triangleq \max(x,0)$ denoting the positive part of x, and $a_{\text{opt}}(f)=0$ for $f\in\mathcal{F}_M\cap(\mathcal{F}_{\lambda_{\max}})^c$.

Proof: See Appendix C. □

The solution found in *Theorem 1* leads to the jointly minimized MSE ε_{opt} given by

$$\varepsilon_{\text{opt}} = \int_{\mathcal{F}_M} \frac{TM(fT)}{1+\frac{M(fT)}{T}\lambda_{\max}(f)a_{\text{opt}}(f)}df. \quad (44)$$

Note that (42) and (43) show that $a_{\text{opt}}(f)$ is a monotone non-decreasing function of the average transmit power $A>0$. Thus, (44) shows that the minimized MSE is a monotone non-increasing function of A, which justifies the use of the equality constraint $\bar{P}=A$ instead of the inequality constraint $\bar{P}\le A$ in the formulation of *Problem 1*.

$\gamma=0.2$, and the length of each guard band is $0.2/T_0$. The overlay systems with $1/T=1/T_0$ are to be designed. For illustrative purpose, the channels to the overlay Rx are chosen to be two-path frequency selective channels with impulse responses $h_1(t)=0.9e^{j\frac{\pi}{4}}\delta(t-T_0/8)+0.4\delta(t-15T_0/16)$, $h_2(t)=0.5e^{-j\frac{\pi}{2}}\delta(t-T_0/2)+0.8e^{j\pi}\delta(t-5T_0/11)$, $h_3(t)=0.7e^{j\pi}\delta(t-T_0/4)+0.9e^{-j\frac{\pi}{2}}\delta(t-T_0/5)$, $h_4(t)=0.3e^{j\frac{23\pi}{40}}\delta(t-T_0/2)+0.6\delta(t-T_0/8)$, and $h(t)=0.7e^{j\frac{\pi}{2}}\delta(t-T_0/4)+0.9e^{j\pi}\delta(t-19T_0/80)$. Fig. 3-(a) shows the PSDs of the legacy and the overlay signals observed at the overlay Rx. The symbol timing offset between the 2nd and the 3rd legacy transmitters is $0.4T_0$, and the received signals are, respectively, $6, 0, 2$, and 4 [dB] stronger than the overlay signal, where the legacy systems are numbered from left to right. The overlay

(i) D=1.22, D_L=1 0.22
(ii) D=2.44, D_L=2, 0.44
(iii) D=4.88, D_L=4, 0.88
(iv) D=9.76 D_L=8. 1.76

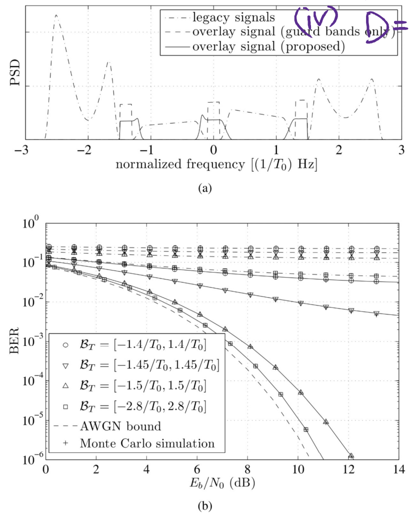

Fig. 3. Comparison of the overlay system that utilizes guard bands only with the proposed scheme. (a) PSDs of the legacy and overlay signals. (b) Average BER versus E_b/N_0 for various transmit bands: (–·) guard bands only, (—) proposed.

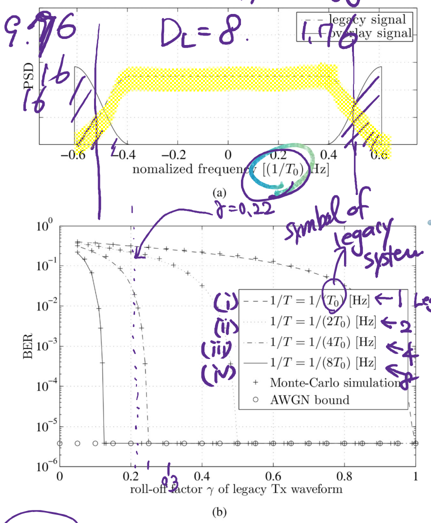

Fig. 4. Trade-off between the average BER and the symbol rate when there is no spectrum hole. (a) PSDs of the user signals when $\gamma=0.22$ and $1/T=1/(4T_0)$. (b) BER versus roll-off factor of the waveform of the legacy Tx.

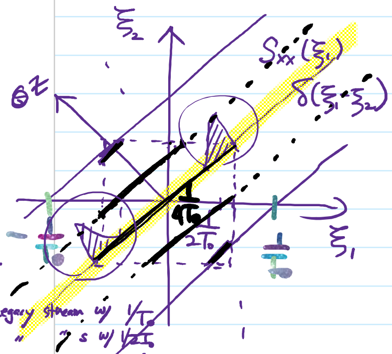

excessive
excess (o)
access (x)

$\Sigma\, b_n\, p(t-nT)$

Nyquist Criterion.
BW of $p(t) \ge \frac{1}{2T}$
$\Leftrightarrow$ $p(t)$ can be a Nyquist pulse.

$P(f)$

system has $E_b/N_0=10$ [dB] and $\mathcal{B}_T=[-1.5/T_0,1.5/T_0]$, and $\mathcal{B}_R=[-3/T_0,3/T_0]$. Note that, even though the PSD of the overlay signal overlaps with those of the legacy signals, the overlay signal does not induce any interference at the legacy receivers. Fig. 3-(b) shows the BER performance of the overlay systems. The receive band is the same as Fig. 3-(a). It can be seen that the performance of the proposed overlay system is significantly better and improves as the length of the transmit band increases, while that of the overlay system that utilizes only the guard bands improves very little.

The next results are to show the trade-off between the BER and the symbol rate of the overlay system. We consider an

and the overlay signals are frequency-shifted, amplified, and retransmitted by a single relay, the bent-pipe satellite, and the terminals can demodulate either the legacy signal, the overlay signal, or both. The LOS channels from the satellite to the receivers are assumed flat and of the same gain. Under this assumption, multiple receivers can be regarded as a pair of co-located legacy and overlay receivers. As the propagation delays from the overlay and the legacy transmitters to a receiver are identical, it turns out that the optimal solution not only makes the overlay signal orthogonal to the legacy receiver but also makes the overlay receiver to completely null out the legacy signal.

As shown in Fig. 4-(b), a better BER performance can system is significantly better and improves as the length of the transmit band increases, while that of the overlay system that utilizes only the guard bands improves very little.

The next results are to show the trade-off between the BER and the symbol rate of the overlay system. We consider an extreme case, where the entire frequency band is occupied by the legacy signal, so that no frequency band free of the legacy signal is available to the overlay system. As shown in Fig. 4-(a), there is one legacy system with the symbol rate of $1/T_0$ [Hz] and $E_b/N_0 = 10$ [dB]. The symbol rate $1/T$ of the overlay Tx is chosen to be a fraction of $1/T_0$, and $\mathcal{B}_T = \mathcal{B}_R = [-(1+\gamma)/(2T_0), (1+\gamma)/(2T_0)]$ [Hz]. A scenario of upgrading a fixed communication link by overlaying another system is considered, where the legacy and the overlay transmitters are located in the same place. If the possible nonlinearity of the satellite amplifier is ignored, this scenario is applicable to satellite broadcasting to multiple terminals over line-of-sight (LOS) channels. The legacy and the overlay transmitters are co-located in a terrestrial station, the legacy receiver are identical, it turns out that the optimal solution not only makes the overlay signal orthogonal to the legacy receiver but also makes the overlay receiver to completely null out the legacy signal.

As shown in Fig. 4-(b), a better BER performance can be achieved by reducing the transmission rate of the overlay system. For example, at $\gamma = 0.25$, the overlay systems with $1/T = 1/(4T_0)$ and $1/(8T_0)$ can achieve the AWGN bound though those with $1/T = 1/T_0$ and $1/(2T_0)$ cannot. This is because, though the legacy signal physically occupies the entire bandwidth of length $(1+\gamma)/(2T_0)$ [Hz], it effectively occupies only $1/(2T_0)$ [Hz] of the total bandwidth and leaves the legacy-free bandwidth of $\gamma/(2T_0)$ [Hz] for the overlay system to shape the transmit pulse. Since $(1+\beta)/(2T) = \gamma/(2T_0)$, with β being the excess bandwidth of the overlay system, if $1/T$ is chosen to result in $\beta \geq 0$, i.e.,

$$\frac{T_0}{T} \leq \gamma, \tag{47}$$

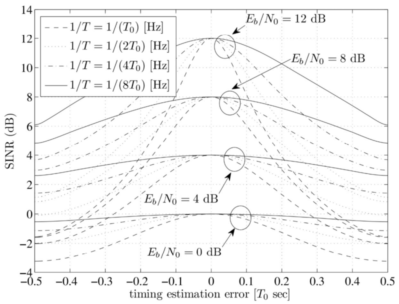

Fig. 5. SINR of the legacy system vs. estimation error in the timing of the legacy receiver for the scenario considered in Fig. 4 with $\gamma = 0.22$.

then the bandwidth $\gamma/(2T_0)$ becomes greater than or equal to the Nyquist bandwidth $1/(2T)$ for the overlay system to have no self-interference. Therefore, whatever small value γ has, the BER performance of the overlay system as low as the AWGN bound is always achievable by reducing the transmission rate, as far as γ is positive.

Fig. 5 illustrates the robustness of the proposed overlay system under the estimation error in the timing of the legacy receiver for the scenario considered in Fig. 4. Under such mismatch, the interference from the overlay system is not perfectly canceled at the output of the legacy receiver. Sixteen combinations of parameters with $E_b/N_0 = 0, 4, 8$, and 12 dB and $T = T_0, 2T_0, 4T_0$, and $8T_0$ are considered, and the SINR of the legacy system is shown as a function of the amount of the mismatch. Fig. 5 combined with Fig. 4 shows that a slower transmission of the overlay data symbols improves not only the BER performance of the overlay system by effectively increasing the bandwidth but also the robustness of the proposed overlay scheme under mismatch by reducing the interference power. For example, under 10% estimation error and E_b/N_0 less than or equal to 12 dB, the SINR degradation

overlay scheme significantly improves the spectral efficiency without requiring any modification of the system parameters of the legacy systems.

Appendix

A. Proof of Lemma 1

Proof: Define $p_k(t) \triangleq s(t) \otimes h_k(t)$. Then, using the Poisson summation formula [21, p. 589] and the definition of $M(f)$ in (1), the left side of (9c) can be rewritten as

$$\sum_{l''=-\infty}^{\infty} m[-l'']\left\{\sum_{l'=-\infty}^{\infty} q_k\left(l'T + \frac{lT}{M_0M_k}\right)\right.$$
$$\left.\cdot q_k\left(l'T + \frac{lT}{M_0M_k} - l''T\right)^*\right\} \tag{48a}$$
$$= \frac{1}{T}\sum_{l'=-\infty}^{\infty}\int_{-\infty}^{\infty} Q_k(\xi)Q_k\left(\xi - \frac{l'}{T}\right)^* e^{j2\pi\frac{ll'}{M_0M_k}} M(\xi T)d\xi \tag{48b}$$
$$= \frac{1}{T}\int_{-\infty}^{\infty} M(\xi T)W_k(\xi)^* e^{j2\pi\xi\left(\tau_k + \frac{lT}{M_0M_k}\right)} P_k(\xi)$$
$$\cdot \sum_{l'=-\infty}^{\infty} P_k\left(\xi - \frac{l'}{T}\right)^* e^{-j2\pi\left(\xi - \frac{l'}{T}\right)\left(\tau_k + \frac{lT}{M_0M_k}\right)} W_k\left(\xi - \frac{l'}{T}\right) d\xi \tag{48c}$$

which is a periodic function of l with period M_0M_k. Thus, it is enough to have (48c) equal to zero for $l = 0, 1, ..., M_0M_k - 1$. Then, using the relation $\boldsymbol{p}_k(f) = \boldsymbol{h}_k(f) \odot \boldsymbol{s}(f)$ and the definition of $\boldsymbol{H}_k(f)$ in (20), (48c) can be rewritten as

$$\int_{\mathcal{F}} \frac{1}{T}\left|\sqrt{M(fT)}\left(\boldsymbol{w}_k(f) \odot \boldsymbol{e}_{k,l}(f)\right)^{\mathcal{H}} \boldsymbol{p}_k(f)\right|^2 df \tag{49a}$$
$$= \int_{\mathcal{F}} \frac{1}{T}\left|\sqrt{M(fT)}\boldsymbol{w}_{k,l}(f)^{\mathcal{H}}\left(\boldsymbol{H}_k(f)\boldsymbol{s}(f)\right)\right|^2 df, \tag{49b}$$

which must be zero $\forall k \in \mathcal{K}, \forall l \in \{0, 1, ..., M_0M_k - 1\}$. A measurable function $f(x)$ equals zero almost everywhere in an interval I iff $\int_I |f(x)|^2 dx = 0$. Moreover, the Fourier transform does not distinguish signals that equal almost everywhere. Therefore, (49b) is equivalent to (18). □

pulse.

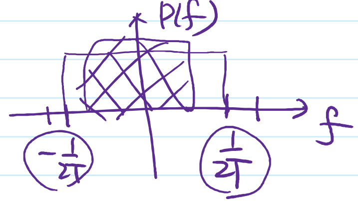

$B \geq \frac{1}{2T}$

$\beta = \frac{B}{\frac{1}{2T}} - 1$

$\Leftrightarrow$ $B = \frac{1+\beta}{2T}$

$\beta = 1 \Rightarrow$ twice the minimum required BW is used in pulse shaping

$\beta \times 100 \Rightarrow 22\%$

Multi-Stream Decomposition of PAM/QAM Signal

(1) $X(t) = A\sum_{n=-\infty}^{\infty} d_n p(t - nT)$

the symbol Tx rate is $1/T$ [symbol/sec].

$= \underbrace{A\sum_{m=-\infty}^{\infty} d_{2m}\, p(t-2mT)}_{\text{symbol Tx rate is } 1/2T} + \underbrace{A\sum_{m=-\infty}^{\infty} d_{2m+1}\, p(t-(2m+1)T)}_{1/2T}$

$= \boxed{A\sum_{m=-\infty}^{\infty}\sum_{l=0}^{2} d_{3m+l}\, p(t-(3m+l)T)}$

not only the BER performance of the overlay system by effectively increasing the bandwidth but also the robustness of the proposed overlay scheme under mismatch by reducing the interference power. For example, under 10% estimation error and E_b/N_0 less than or equal to 12 dB, the SINR degradation is around maximum 4 dB for $T = T_0$ but it is less than 1.5 dB for $T = 4T_0$ and $T = 8T_0$.

VI. Conclusions

In this paper, we have considered the design of an overlay system in a WSCS legacy signal. The optimal transmit and receive waveforms of the overlay system are derived that jointly minimize the MSE at the output of the linear receiver of the overlay system, subject to zero interference at the output samples of the legacy receivers. Using the VFT technique, the optimal continuous-time band-limited solution and the necessary and sufficient condition for the existence of the optimal solution are derived in the frequency domain. The notion of virtual legacy receivers is introduced to allow non-identical transmit and receive bands, and the rate reduction of the overlay system is taken into account in the derivation of the solution to allow trade-off between the transmission rate and the performance. It is shown that the proposed orthogonal

A measurable function $f(x)$ equals zero almost everywhere in an interval I iff $\int_I |f(x)|^2 dx = 0$. Moreover, the Fourier transform does not distinguish signals that equal almost everywhere. Therefore, (49b) is equivalent to (18). □

B. Proof of Proposition 1

Proof: Let $\hat{\boldsymbol{B}}(f)^{\mathcal{H}}$ be a matrix that consists of the basis vectors of the row space of $\boldsymbol{B}(f)^{\mathcal{H}}$. Then, the orthogonality constraint can be rewritten as $\hat{\boldsymbol{B}}(f)^{\mathcal{H}}\boldsymbol{s}(f) = \boldsymbol{0}$. Now, define the Lagrangian function as

$$\mathcal{L}(\boldsymbol{s}(f), \lambda(f), \boldsymbol{\mu}(f)) \triangleq \boldsymbol{s}(f)^{\mathcal{H}}\boldsymbol{C}(f)\boldsymbol{s}(f) \\ -\lambda(f)\big(\boldsymbol{s}(f)^{\mathcal{H}}\boldsymbol{s}(f) - a(f)\big) + 2\Re\left(\boldsymbol{s}(f)^{\mathcal{H}}\hat{\boldsymbol{B}}(f)\boldsymbol{\mu}(f)\right) \quad (50)$$

by introducing the real- and the complex-valued Lagrange multipliers $\lambda(f)$ and $\boldsymbol{\mu}(f)$, respectively. By taking the gradient with respect to $\boldsymbol{s}(f)$ and setting it to zero, we have

$$\boldsymbol{0} = \boldsymbol{C}(f)\boldsymbol{s}(f) - \lambda(f)\boldsymbol{s}(f) + \hat{\boldsymbol{B}}(f)\boldsymbol{\mu}(f) \quad (51a)$$
$$= \hat{\boldsymbol{B}}(f)^{\mathcal{H}}\boldsymbol{C}(f)\boldsymbol{s}(f) + \hat{\boldsymbol{B}}(f)^{\mathcal{H}}\hat{\boldsymbol{B}}(f)\boldsymbol{\mu}(f), \quad (51b)$$

where we pre-multiply $\hat{\boldsymbol{B}}(f)^{\mathcal{H}}$ to (51a) and use the orthogonality constraint to obtain (51b), which leads to $\boldsymbol{\mu}(f) =$

$-\big(\hat{\boldsymbol{B}}(f)^{\mathcal{H}}\hat{\boldsymbol{B}}(f)\big)^{-1}\hat{\boldsymbol{B}}(f)^{\mathcal{H}}\boldsymbol{C}(f)\boldsymbol{s}(f)$. Substituting this back to (51a), we have

$$\boldsymbol{P}_{\hat{\boldsymbol{B}}}^{\perp}(f)\boldsymbol{C}(f)\boldsymbol{s}(f) = \lambda(f)\boldsymbol{s}(f), \quad (52)$$

where $\boldsymbol{P}_{\hat{\boldsymbol{B}}}^{\perp}(f) = \boldsymbol{I}_{\mathcal{N}(f)} - \hat{\boldsymbol{B}}(f)\big(\hat{\boldsymbol{B}}(f)^{\mathcal{H}}\hat{\boldsymbol{B}}(f)\big)^{-1}\hat{\boldsymbol{B}}(f)^{\mathcal{H}}$ is the projection matrix, which can be alternately written as (36b). This necessary condition is satisfied by all eigenvector-eigenvalue pairs of $\boldsymbol{P}_{\hat{\boldsymbol{B}}}^{\perp}(f)\boldsymbol{C}(f)$. Let $\boldsymbol{v}(f)$ be an eigenvector. Then, by pre-multiplying $\boldsymbol{P}_{\hat{\boldsymbol{B}}}^{\perp}(f)$ to (52) and using $\boldsymbol{P}_{\hat{\boldsymbol{B}}}^{\perp}(f)^2 = \boldsymbol{P}_{\hat{\boldsymbol{B}}}^{\perp}(f)$, we have $\boldsymbol{P}_{\hat{\boldsymbol{B}}}^{\perp}(f)\boldsymbol{v}(f) = \boldsymbol{v}(f)$. This implies that, to maximize $\boldsymbol{v}(f)^{\mathcal{H}}\boldsymbol{C}(f)\boldsymbol{v}(f)$, we just need to maximize $\boldsymbol{v}(f)^{\mathcal{H}}\boldsymbol{P}_{\hat{\boldsymbol{B}}}^{\perp}(f)\boldsymbol{C}(f)\boldsymbol{v}(f) = \lambda_{\max}(f)\boldsymbol{v}(f)^{\mathcal{H}}\boldsymbol{v}(f)$, subject to the power constraint (35c). Therefore, the conclusion follows. □

C. Proof of Theorem 1

Proof: For $f \in (\mathcal{F}_M)^c$, $\boldsymbol{s}_{\text{opt}}(f)$ can be chosen arbitrarily, as already mentioned. For $f \in \mathcal{F}_M \cap (\mathcal{F}_{\lambda_{\max}})^c$, $\lambda_{\max}(f) = 0$ implies $a_{\text{opt}}(f) = 0$ and, consequently, $\boldsymbol{s}_{\text{opt}}(f) = 0$, otherwise the energy of the transmit waveform is wasted without contributing to the improvement of the objective function of *Sub-Problem 2*. For $f \in \mathcal{F}_M \cap \mathcal{F}_{\lambda_{\max}}$, $M(fT) \neq 0$ and $\lambda_{\max}(f) \neq 0$ enable the application of the Karush-Kuhn-Tucker condition to find the solution, as *Theorems 3* and *4* in [11]. Therefore, by combining (29) with the solutions for these three different cases, we obtain the jointly optimal solution to *Problem 2* as (40)–(43). □

D. Proof of Lemma 2

Proof: Let $\mathcal{N}'(f)$ be the number of zero entries in $\boldsymbol{h}(f)$ at f. Then, there exists an $\mathcal{N}(f)$-by-$\mathcal{N}(f)$ permutation matrix $\boldsymbol{E}(f)$ such that $\boldsymbol{E}(f)\boldsymbol{h}(f)$ has zeros only at the last

E. Proof of Theorem 2

Proof: From (44), we can see that a non-trivial optimal solution exists iff the length of the set $\mathcal{F}_M \cap \mathcal{F}_{\lambda_{\max}}$ is greater than zero and $a_{\text{opt}}(f)$ is not a zero function on this set. It is clear that $a_{\text{opt}}(f)$ cannot be a zero function on the set, otherwise the power constraint (34) with $A > 0$ is violated. Thus, a non-trivial optimal solution exists iff the length of the set $\mathcal{F}_M \cap \mathcal{F}_{\lambda_{\max}}$ is greater than zero. By the definition of $\lambda_{\max}(f)$ in *Proposition 1*, $\lambda_{\max}(f) > 0$ iff $\boldsymbol{P}_{\boldsymbol{B}}^{\perp}(f)\boldsymbol{C}(f)\boldsymbol{P}_{\boldsymbol{B}}^{\perp}(f) \neq \boldsymbol{0}$, which is equivalent to $\boldsymbol{P}_{\boldsymbol{B}}^{\perp}(f) \neq \boldsymbol{0}$ by *Lemma 2*. Moreover, $\boldsymbol{P}_{\boldsymbol{B}}^{\perp}(f) \neq \boldsymbol{0}$ iff $\text{Dim}\big(\text{null space of } \boldsymbol{B}(f)^{\mathcal{H}}\big) \neq 0$ by (36b). Thus, the set $\mathcal{F}_M \cap \mathcal{F}_{\lambda_{\max}}$ is equal to (46). Therefore, the conclusion follows. □

References

[1] W. A. Gardner and L. E. Franks, "Characterization of cyclostationary random signal processes," *IEEE Trans. Inf. Theory*, vol. 21, pp. 4-14, Jan. 1975.

[2] W. A. Gardner, Ed.,*Cyclostationarity in Communications and Signal Processing*. New York: IEEE Press, 1994.

[3] W. A. Gardner, A. Napolitano, and L. Paura, "Cyclostationarity: half a century of research," *Signal Process.*, vol 86, no. 4, pp. 639-697, Apr. 2006.

[4] J. Salz, "Digital transmission over cross-coupled linear channels," *ATT Tech. J.*, vol. 64, no. 6, pp. 1147-1159, July-Aug. 1985.

[5] G. Golden, J. Mazo, and J. Salz, "Transmitter design for data transmission in the presence of a data-like interferer," *IEEE Trans. Commun.*, vol. 43, no. 2-4, pp. 837-850 , Feb.-Apr. 1995.

[6] P. S. Kumar and S. Roy, "Optimization for crosstalk suppression with noncoordinating users," *IEEE Trans. Commun.*, vol. 44, no. 7, pp. 894-905, July 1996.

[7] J. Yang and S. Roy, "On joint transmitter and receiver optimization for multiple-input-multiple-output (MIMO) transmission systems," *IEEE Trans. Commun.*, vol. 42, no. 12, pp. 3221-3231, Dec. 1994.

[8] J. H. Cho and W. Gao, "Continuous-time equivalents of Welch bound equality sequences," *IEEE Trans. Inf. Theory*, vol. 51, no. 9, pp. 3176-3185, Sep. 2005.

[9] J. H. Cho, "Multi-user constrained water-pouring for continuous-time overloaded Gaussian multiple-access channels," *IEEE Trans. Inf. Theory*, vol. 54, no. 4, pp. 1437-1459, Apr. 2008.

[10] H. S. Mir and S. Roy, "Optimum transmitter/receiver design for a narrowband overlay in noncoordinated subscriber lines," *IEEE Trans. Commun.*, vol. 52, no. 6, pp. 992-998, June 2004.

$= \left[A \sum_{m=-\infty}^{\infty} \sum_{\ell=0}^{2} d_{3m+\ell}\, p(t-(3m+\ell)T) \right]$

ℓ

$1/3T$

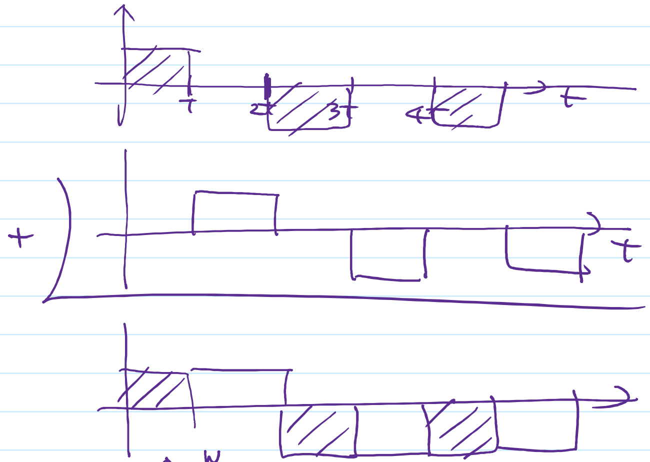

$1/2T$

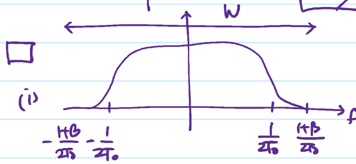

(i) $-\frac{1+\beta}{2T_0}$ $-\frac{1}{2T_0}$ $\frac{1}{2T_0}$ $\frac{1+\beta}{2T_0}$

$\cancel{\frac{1}{T_0}}$

$\frac{1}{T_0}$

$\frac{2\frac{1+\beta}{2T_0}}{\frac{1}{T_0}} = 1+\beta$

(1-D is occupied by legacy.
β-D

0.22

(ii) $\frac{1}{2T_0}$ $\frac{2\frac{1+\beta}{2T_0}}{\frac{1}{2T_0}} = 2+2\beta$

(2-D is " " "
2β-D

0.44

(iii) $\frac{1}{4T_0}$ $= 4+4\beta$

(4-D " " " "
4β-D

0.88

(iii) $\frac{1}{5T_0}$ $\frac{1}{6T_0}$

(iv) $\frac{1}{8T_0}$ $\frac{1}{7T_0}$ $= 8+8\beta$

(8-D " " " "
8β

1.76

16, 16

(I)

□ PAM/QAM signals

$X(t) = A\sum_{n=-\infty}^{\infty} d_n\, p(t-nT)$

D. Proof of Lemma 2

Proof: Let $\mathcal{N}'(f)$ be the number of zero entries in $\boldsymbol{h}(f)$ at f. Then, there exists an $\mathcal{N}(f)$-by-$\mathcal{N}(f)$ permutation matrix $\boldsymbol{E}(f)$ such that $\boldsymbol{E}(f)\boldsymbol{h}(f)$ has zeros only at the last $\mathcal{N}'(f)$ entries. By the positive definiteness of $\boldsymbol{R}_N(f)$ and by definitions (30) and (31), $\boldsymbol{E}(f)\boldsymbol{C}(f)\boldsymbol{E}(f)^{\mathcal{H}}$ can be written as

$$\boldsymbol{E}(f)\boldsymbol{C}(f)\boldsymbol{E}(f)^{\mathcal{H}} = \begin{bmatrix} \hat{\boldsymbol{C}}(f) & \boldsymbol{0} \\ \boldsymbol{0} & \boldsymbol{0} \end{bmatrix} \tag{53}$$

for some positive definite $(\mathcal{N}(f) - \mathcal{N}'(f))$-by-$(\mathcal{N}(f) - \mathcal{N}'(f))$ matrix $\hat{\boldsymbol{C}}(f)$. Note that, by definitions (27) and (36b), all the entries in the ith row and the ith column of $\boldsymbol{P}_{\boldsymbol{B}}^{\perp}(f)$ are zero if the ith entry of $\boldsymbol{h}(f)$ is zero. Thus, $\boldsymbol{E}(f)\boldsymbol{P}_{\boldsymbol{B}}^{\perp}(f)\boldsymbol{E}(f)^{\mathcal{H}}$ can be written as

$$\boldsymbol{E}(f)\boldsymbol{P}_{\boldsymbol{B}}^{\perp}(f)\boldsymbol{E}(f)^{\mathcal{H}} = \begin{bmatrix} \hat{\boldsymbol{P}}_{\boldsymbol{B}}^{\perp}(f) & \boldsymbol{0} \\ \boldsymbol{0} & \boldsymbol{0} \end{bmatrix} \tag{54}$$

for some $(\mathcal{N}(f)-\mathcal{N}'(f))$-by-$(\mathcal{N}(f)-\mathcal{N}'(f))$ matrix $\hat{\boldsymbol{P}}_{\boldsymbol{B}}^{\perp}(f)$. Since $\boldsymbol{E}(f)$ is a permutation matrix, $\boldsymbol{P}_{\boldsymbol{B}}^{\perp}(f)\boldsymbol{C}(f)\boldsymbol{P}_{\boldsymbol{B}}^{\perp}(f) = \boldsymbol{0}$ iff $\boldsymbol{E}(f)\boldsymbol{P}_{\boldsymbol{B}}^{\perp}(f)\boldsymbol{C}(f)\boldsymbol{P}_{\boldsymbol{B}}^{\perp}(f)\boldsymbol{E}(f)^{\mathcal{H}} = \boldsymbol{0}$. Thus, we have $\boldsymbol{P}_{\boldsymbol{B}}^{\perp}(f)\boldsymbol{C}(f)\boldsymbol{P}_{\boldsymbol{B}}^{\perp}(f) = \boldsymbol{0}$ iff $\hat{\boldsymbol{P}}_{\boldsymbol{B}}^{\perp}(f)\hat{\boldsymbol{C}}(f)\hat{\boldsymbol{P}}_{\boldsymbol{B}}^{\perp}(f) = \boldsymbol{0}$. Moreover, $\hat{\boldsymbol{P}}_{\boldsymbol{B}}^{\perp}(f)\hat{\boldsymbol{C}}(f)\hat{\boldsymbol{P}}_{\boldsymbol{B}}^{\perp}(f) = \boldsymbol{0}$ iff $\hat{\boldsymbol{P}}_{\boldsymbol{B}}^{\perp}(f) = \boldsymbol{0}$ by the positive definiteness of $\hat{\boldsymbol{C}}(f)$. Note that $\hat{\boldsymbol{P}}_{\boldsymbol{B}}^{\perp}(f) = \boldsymbol{0}$ iff $\boldsymbol{P}_{\boldsymbol{B}}^{\perp}(f) = \boldsymbol{0}$ by (54). Therefore, the conclusion follows. □

3185, Sep. 2005.

[9] J. H. Cho, "Multi-user constrained water-pouring for continuous-time overloaded Gaussian multiple-access channels," *IEEE Trans. Inf. Theory*, vol. 54, no. 4, pp. 1437-1459, Apr. 2008.

[10] H. S. Mir and S. Roy, "Optimum transmitter/receiver design for a narrowband overlay in noncoordinated subscriber lines," *IEEE Trans. Commun.*, vol. 52, no. 6, pp. 992-998, June 2004.

[11] J. H. Cho, "Joint transmitter and receiver optimization in additive cyclostationary noise," *IEEE Trans. Inf. Theory*, vol. 50, no. 14, pp. 3396-3405, Dec. 2004.

[12] T. Berger and D. W. Tufts, "Optimum pulse amplitude modulation—part I: transmitter-receiver design and bounds from information theory," *IEEE Trans. Inf. Theory*, vol. IT-13, no. 2, pp. 196-208, Apr. 1967.

[13] G. Strang, *Linear Algebra and its Applications*, 4th edition. Pacific Grove, CA: Brooks Cole, 2005.

[14] S. Boyd and L. Vandenberghe, *Convex Optimization*. New York: Cambridge Univ. Press, 2004.

[15] J. Farserotu and R. Prasad, "A survey of future broadband multimedia satellite systems, issues and trends," *IEEE Commun. Mag.*, vol. 38, no. 6, pp. 128-133, June 2000.

[16] A. Scaglione, P. Stoica, S. Barbarossa, G. B. Giannakis, and H. Sampath, "Optimal design for space-time linear precoders and decoders," *IEEE Trans. Signal Process.*, vol. 50, no. 5, pp. 1051-1064, May 2002.

[17] J. H. Cho and J. S. Lehnert, "An optimal signal design for band-limited asynchronous DS-CDMA communications," *IEEE Trans. Inf. Theory*, vol. 48, no. 5, pp. 1172-1185, May 2002.

[18] G. H. Golub, "Some modified matrix eigenvalue problems," *SIAM Review*, vol. 15, no. 2, part 1, pp. 318-334, Apr. 1973.

[19] Z. Bai and G. H. Golub, "Some unusual matrix eigenvalue problems," *SCCM Tech. Rep.*. [Online]. Available: http://www-sccm.stanford.edu/nf-publications-tech.html, SCCM-98-12, 1998.

[20] Y. K. Jeong, J. H. Cho, and J. S. Lehnert, "An asymptotic analysis of band-limited DS/SSMA communication systems," *IEEE Trans. Inf. Theory*, vol. 52, no. 2, pp. 759-766, Feb. 2006.

[21] J. G. Proakis, *Digital Communications*, 4th edition. New York: McGraw Hill, 2001.

Yeo Hun Yun (S'09) received the B.S. degree (summa cum laude) in Information, Communication, and Electronics Engineering from Catholic University, Korea, in 2006 and the M.S. degree in Computer and Communications Engineering in 2009 from Pohang University of Science and Technology (POSTECH), Pohang, Korea, where he is currently working toward the Ph.D. degree. His research interests include cognitive radio and multiuser communications.

Joon Ho Cho (S'99-M'01) received the B.S. degree (summa cum laude) in Electrical Engineering from Seoul National University, Seoul, Korea, in 1995 and the M.S.E.E. and Ph.D. degrees in Electrical and Computer Engineering from Purdue University, West Lafayette, IN, in 1997 and 2001, respectively.

From 2001 to 2004, he was with the University of Massachusetts at Amherst as an Assistant Professor. Since July 2004, he has been with Pohang University of Science and Technology (POSTECH), Pohang, Korea, where he is presently an Associate Professor in the Department of Electronic and Electrical Engineering. His research interests include wideband systems, multiuser communications, adaptive signal processing, channel measurement and modeling, and information theory.

Dr. Cho served as an Associate Editor for the IEEE TRANSACTIONS ON VEHICULAR TECHNOLOGY.

□ PAM/QAM signals

$X(t) = A\sum_{n=-\infty}^{\infty} d_n\, p(t-nT)$

□

$\tilde{X}(t) = A\sum_{l=0}^{3}\sum_{m=-\infty}^{\infty} d_{4m+l}\, p_l(t-(4m+l)T)$

4 PAM/QAM

$p_0(t)$ $p_1(t)$ $p_2(t)$ $p_3(t)$

... d_0 d_1 d_2 d_3

d_4 d_5 d_6 d_7

...

$1/4T$

□ Square QAM = multiple BPSK

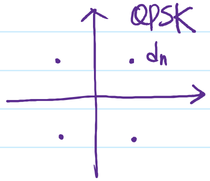

$d_n = b_{I,n} + j\, b_{Q,n}$ $b_{I,n}, b_{Q,n} \in \{1, -1\}$

$A\sum_n d_n\, p(t-nT) = A\sum b_{I,n}\, p(t-nT) + \tilde{A}\sum b_{Q,n}\, j p(t-nT)$

$p(t)$ $g(t) \triangleq j p(t) \neq p(t)$

$A = \tilde{A}$

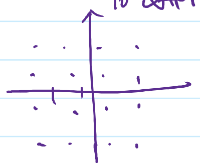

$d_n = b_{I,n} + j\, b_{Q,n}$ $b_{I,n}\ b_{Q,n} \in \{-3, -1, 1, 3\}$ 4-PAM